Evolution of polygonal patterns in stratified mud during desiccation: The role of flaw distribution and layer boundaries

Ram Weinberger*
Geological Survey of Israel, 30 Malkhe Israel Street, Jerusalem 95501, Israel

ABSTRACT

Detailed analysis of diagnostic surface morphologies of fractures in natural mud indicates that mud cracks systematically nucleate at the bottom of the mud and propagate vertically upward toward the free surface and laterally outward toward adjacent cracks. Earlier generations of mud cracks rupture the set of desiccated layers altogether, forming polygonal patterns that are similar throughout the mud sequence. Later generations of mud cracks subdivide each layer separately, forming markedly different polygonal patterns within individual mud layers. A simple mechanical model draws an analog between cooling of granular materials and drying of mud. It shows that subfact defects at grain boundaries near the base may become critical before defects associated with fine particles at the top, even though the stress profile due to drying is usually more tensile at the top. Thin-section analysis and sieving method indicate that grain boundaries at the bottom are several times longer than at the top of the mud due to the natural sorting of grains, illustrating the validity of the model. This study suggests that stress variations with depth are less important for pattern evolution of mud cracks than previously theorized. However, nonuniform flaw distribution and surface discontinuities play a fundamental role during mud-crack nucleation and growth. These results have significance for several subjects, including experimental studies of cracking induced by desiccation, the previously suggested analogy between natural mud fracturing and basalt fracturing, and the use of mud cracks in stratigraphic interpretation.

*E-mail: rami@earth.es.huji.ac.il.

Keywords: joints, mud, mud cracks, nucleation, polygonal fractures.

INTRODUCTION

Field observations and laboratory experiments on natural rocks and rock-like materials indicate that fractures nucleate at some type of flaw. They do so because flaws and defects in the material amplify the remote stress, causing the local tensile stress at the defect to exceed the tensile strength of the material. Examples of flaws are preexisting microcracks, holes, grain boundaries, and irregularly shaped grains located throughout the specimen or rock mass. The flaws of interest are those that happen to be located in an area being stressed highly enough that a small increase in the local stress field results in a fracture. Such flaws may be favorably located along layer boundaries in sedimentary rocks (Bahat and Engelder, 1984; Helgeson and Aydin, 1991) and at interfaces in composite materials (Piggott, 1991), where maximum remote stress may concentrate and interface strength be reduced (Kranz, 1983; Bahat, 1991; Ji and Zhao, 1994). These surface discontinuities also have a strong effect on the propagation paths and terminations of the recently nucleated fractures (e.g., Gross, 1993). Thus, flaws and surface discontinuities play a fundamental role during crack nucleation and growth in layered materials.

The formation of a set of mud layers in which the grain size increases with depth is a ubiquitous phenomenon that is commonly observed on drying puddles, river flood plains, and lake margins during droughts (Allen, 1985; Weinberger, 1999). Cracking of mud layers during loss of moisture forms arrays of joints, known as mud cracks or desiccation cracks. In plan view, mud cracks form remarkable polygonal patterns (Fig. 1) that have been extensively described in the geological literature (Allen, 1985, and references therein). Cracking of mud, which involves a substantial volume loss, is evidently very different from cracking of ordinary rock masses. Nevertheless, the principles of fracture mechanics of solid materials apply to many cracking phenomena in mud (Scott, 1963; Pollard and Aydin, 1988; Lawn, 1993; Müller, 1998). For example, mud cracks typically intersect at right angles (Fig. 1). This is because the first opening-mode crack produces two traction-free surfaces; a second crack tends to approach the first crack orthogonally to these surfaces in order to satisfy these boundary conditions (Lachenbruch, 1962).

Mud cracks have generally been theorized as downward-propagating fracture planes that nucleate at or near the surface and terminate at depth (Neal et al., 1968; Selley, 1976), because the rate of moisture loss apparently declines downward through the layers, as does the tensile stress (Allen, 1985). In this scenario, a newly formed crack nucleates at the surface where the tensile stress due to drying is maximal; subsequently, it propagates downward to the level in which the horizontal stress acting within the mud becomes compressive as a result of the weight of the overlying mud mass. Naturally, surface defects such as bird's footprints (Plummer and Gostin, 1981), gastropod trails (Baldwin, 1974), and raindrops (Fig. 2) are all associated with near-surface initiation and downward growth of mud cracks. However, Weinberger (1999) showed that in the absence of surface defects, cracks consistently nucleate along or near the base of the mud and subsequently propagate upward toward the free surface (Fig. 1).

Fine mud is not the only substance in which contraction gives rise to polygonal patterns. Such patterns also appear during drying in other materials such as plaster, coffee-water mixtures (Groisman and Kaplan, 1994), and starch-water mixtures (Walker, 1986; Müller, 1998), as well as during thermal contraction in basalt flows (Ryan and Sammis, 1978; Ay-

GSA Bulletin; January 2001; v. 113; no. 1; p. 20–31; 10 figures; 1 table.

din and DeGraff, 1988; Grossenbacher and McDuffie, 1995) and in permafrost regions (Lachenbruch, 1962). While the mechanical properties and chemistry of these materials are very different from that of mud, it is tempting to generalize the mechanism driving the polygonal pattern evolution in all of these materials (e.g., Groisman and Kaplan, 1994). Müller (1998) suggested an analogy between basalt cooling and starch desiccation: water concentration in the starch behaves as temperature does in the basalt (quantities obey diffusion equations; water loss is equivalent to heat loss); the resulting contraction stress has a similar dependence on depth and time, and in both cases the material strength is exceeded upon cracking.

This study examines the validity of this analogy in light of detailed observations of polygonal pattern evolution in natural mud. The objective is to elucidate the roles of nonuniform flaw distribution and layer boundaries on the nucleation and three-dimensional growth of mud cracks. This study takes advantage of the well-developed surface morphology of mud cracks (Figs. 1 and 2) and expands my observations (Weinberger, 1999) to multilayered mud. I develop a comprehensive mechanical model wherein mud cracks nucleate at depth and propagate upward and outward in layered mud, and discuss the significance of this mechanism to our understanding of crack growth during contraction in other materials and geological environments.

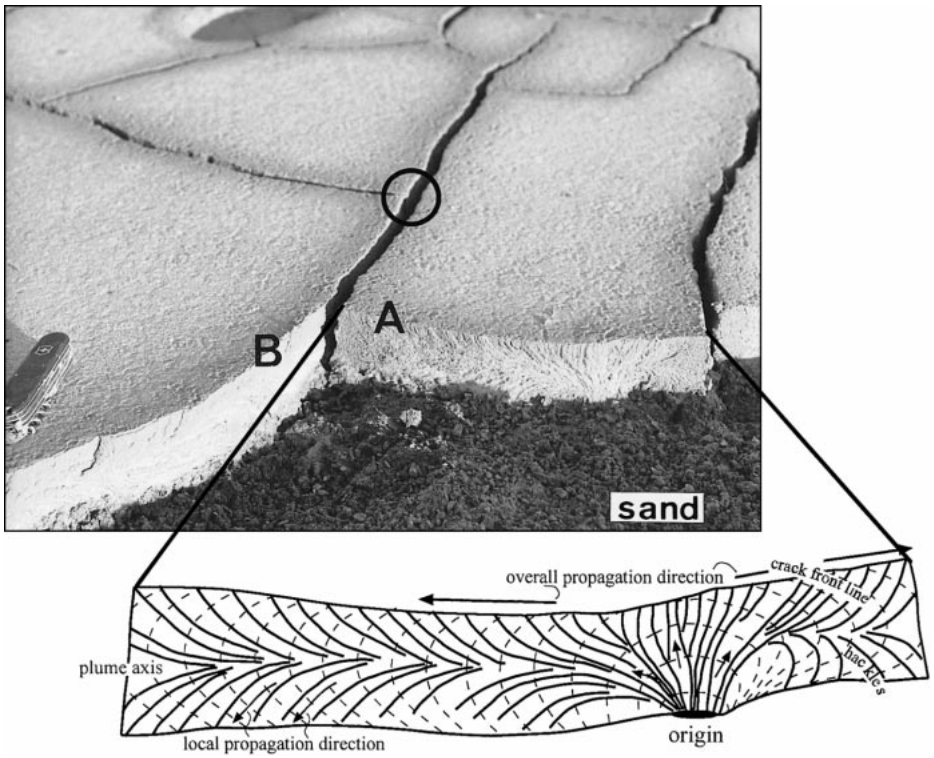

Figure 1. Oblique view of crack walls in desiccated mud at the foot of Massada, Dead Sea region, Israel. Circle shows an orthogonal intersection (T junction). The termination of a new crack (A) is against the plane of an older through-going crack (B). Uncracked sandy substance underlying the mud is seen in the front of the photograph. The wall of crack A is optimally illuminated and shows diagnostic surface morphology. Illustration below shows the use of this morphology to interpret crack origin, local and overall propagation directions (solid arrows), and past crack front (broken lines). Knife is 90 mm long.

THEORETICAL CONSIDERATIONS

Natural mud is far too complicated for the tensile stress created within it during persistent desiccation to be predicted mathematically. Some insight can be gained by drawing an analogy between thermal stress in a cooling elastic layer and stress due to contraction in a drying layer (Müller, 1998). Temperature change ΔT in an unconstrained material produces a volume change ΔV such that (Turcotte and Schubert, 1982, equation 4-171)

$$\left(\frac{\Delta V}{V}\right)_{un} = -\alpha_v \Delta T, \qquad (1)$$

where α_v is the volumetric coefficient of thermal expansion. The temperature change $\Delta T = T_0 - T(z, t)$ is measured relative to the solidus temperature of basalt T_0, where $T(z, t)$ is a depth- and time-dependent temperature profile. For defined conditions of no horizontal strain the volume change is (Müller, 1998)

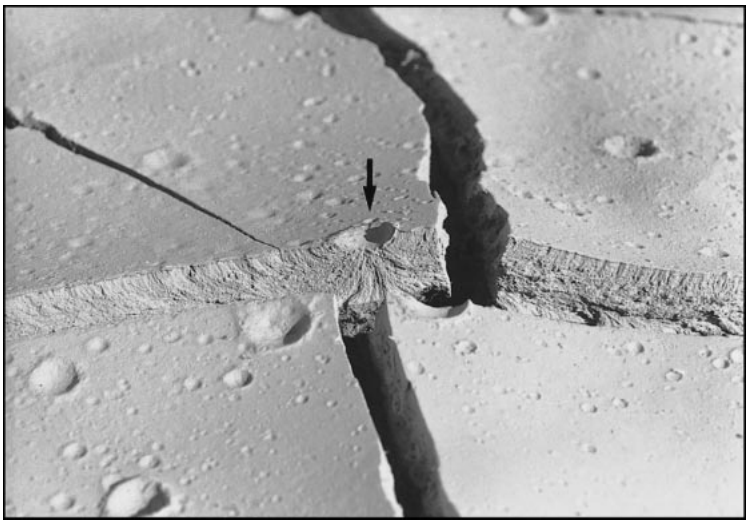

Figure 2. Nucleation of mud cracks associated with raindrop impressions. Hackles radiating away from an impression (arrow) indicate that the crack ruptures the desiccated mud layer before it significantly propagates laterally. Raindrop diameter is 10 mm.

$$\frac{\Delta V}{V} = \frac{1 + \nu}{3(1 - \nu)}\left(\frac{\Delta V}{V}\right)_{un}, \qquad (2)$$

where ν is Poisson's ratio. The horizontal principal thermal stresses for a uniform elastic material, assuming plane stress conditions ($\sigma_z = 0$) are α_v (Lachenbruch, 1962, equation 9; Turcotte and Schubert, 1982, equation 4-186):

$$\sigma_x = \sigma_y = \frac{E\alpha_l \Delta T}{1 - \nu} = \frac{E\alpha_v T}{3(1 - \nu)}, \qquad (3)$$

where E is Young's modulus, $\alpha_l = \alpha_v/3$ is the linear coefficient of thermal expansion, and positive stress values denote tension. Substituting equations 1 and 2 into equation 3 relates the thermal stress to the volume change.

By analogy to thermal stress, the tensile stress due to contraction of a drying layer under the preceding assumptions is (after Müller, 1998):

$$\sigma_x = \sigma_y = \frac{E[C_0 - C(z, t)]}{3(1 - \nu)}, \qquad (4)$$

where $C(z, t)$ is the depth- and time-dependent, dimensionless moisture concentration profile in mud, and C_0 is the initial value of C. Müller (1998) suggested that $C(z, t)$ plays the same role during desiccation as the temperature profile $T(z, t)$ during cooling. The profile $C(z, t)$ in a drying layer is more difficult to compute than $T(z, t)$, mainly because the concentration of water is strongly influenced by newly formed cracks. However, at any time ($C_0 - C$) is higher at the top than at the bottom and decreases with depth as does the horizontal tensile stress (Müller and Dahm, 2000).

Allen (1985) suggested that tensile stress due to surface tension in wet sediment accounts for the continued shrinkage of the mud. In his two-dimensional model, the sediment is composed of straight cylindrical grains of uniform diameter D arranged parallel to each other. The tensile stress perpendicular to a plane between two grains is (Allen, 1985):

$$\sigma_x = \frac{2P \sin\delta}{D}, \qquad (5)$$

where P is the surface tension per unit cylinder length and δ is an angle subtended by the meniscus edges at the grain centers. The normal stress is directly proportional to the surface tension and inversely proportional to the grain size. The angle δ varies to the value $\delta = \pi/4$ radians when the grains become entirely surrounded by water. Thus in natural mud, the tensile stress should be higher at the top than at the bottom due to the fining upward of grain size. This stress would build gradually, increasing with progressive moisture loss to a maximum, as menisci appear in increasingly small pore space.

The preceding analysis indicates that the top of the desiccated material is subjected to higher tensile stress than the bottom due to drying. This led Allen (1985) to predict that cracks would nucleate at the surface of the desiccated mud and grow downward. This prediction is confirmed for a homogeneous starch-water mixture (Müller, 1998, his Plate 3a). However, careful measurements by Corte and Higashi (1960, their Fig. 11) in soil show that the moisture content profile does not vary much with depth at the approximate time when the cracking starts in the experiments. Consequently, in a layered, heterogeneous, size-sorted material such as mud, it is unlikely that the stress profile alone governs the crack origin points in natural mud. In natural sediment, discontinuities such as flaws and layer boundaries serve as preferential nucleation sites for fractures. Their role in the formation of crack patterns in mud therefore deserves careful consideration.

EVOLUTION OF POLYGONAL PATTERNS IN NATURAL MUD

Setting and Methods

The fracture characteristics of mud cracks were mainly studied in dehydrating mud puddles in the Dead Sea region, Israel. Thin-section analysis indicates that the layered mud consists of clay with particles of carbonate, gypsum, chert, ore, quartz, and diatoms derived from the nearby Lisan Formation (Begin et al., 1974). Grain-size distribution displays fining upward (sorting effect) and stratification (Fig. 3). There is a distinct surface discontinuity between the upper desiccated layers, which tend to contract and crack, and the uncracked lower layers. This surface is hereafter referred to as the bottom of the mud. A surface discontinuity is also evident between the desiccated layers (Fig. 4B). Crack-origin points, propagation directions, and terminations were interpreted by studying the well-developed surface morphology of natural mud cracks (Fig. 1). To infer the order of crack formation at a given intersection, the following useful criteria are applied (Fig. 1; Kulander et al., 1979; Aydin and DeGraff, 1988): (1) the origin of a new crack is along the periphery of an older crack; and (2) the termination of a new crack is against the plane of an older through-going crack. Two en echelon cracks with curved overlapping paths are most likely formed during simultaneous propagation of adjacent cracks (Pollard and Aydin, 1988; Olson and Pollard, 1989).

Nucleation and Growth in Multilayered Mud

Cracks originate at or near layer boundaries and rarely along other crack surfaces. Earlier generations of mud cracks originate along the bottom of the mud and seldom along boundaries between the desiccated layers, but later generations commonly originate along such boundaries. Soon after initiation at their origins, cracks rupture the desiccated layers altogether and subsequently extend laterally (Figs. 1 and 4). In plan view, the cracks may follow straight or curved paths, dividing the sediments into thin cells (polygons). The crack walls show several types of surface morphology (see details in Weinberger, 1999), the most typical being an asymmetric plumose structure about a curved plume axis (Fig. 4). The plume axis is vertically oriented perpendicular to bedding near the bottom, then gradually curves close to a certain boundary between the desiccated layers, and may align with the boundary between these layers. For these cracks, the lower and upper vertical terminations are, respectively, an intersection between the crack and the underlying sandy bottom, and an intersection between the crack and the free surface. For mud cracks of a later generation that rupture single or multiple desiccated layers, the vertical terminations are an intersection between the crack and the adjacent layer interface. The lateral terminations of a crack are usually an intersection between two adjacent cracks, but lateral blind terminations of nonintersecting adjacent cracks with curved overlapping paths are not uncommon.

Persistent desiccation leads to continuous fracturing and delaminating of the set of mud layers. At this stage, evolution of polygonal patterns is restricted to certain layers, each of which forms a different polygonal pattern than the neighboring layers. This pattern evolution is documented during sequential removal of mud layers from the top to bottom of a single polygon (Fig. 5). Persistent desiccation, however, usually severely damages the fragile plumose structures, impeding precise identification of all the crack-origin points in each layer separately.

Polygon Sides

Of 68 polygons studied in detail, 2 adjacent polygons are presented in Figure 4A. The number of sides of polygon A as seen in plan view is not clear (three sides? four sides?). Careful examination of the walls of this polygon (Fig. 4B) reveals that it consists of only two bounded cracks, which formed by two single fracture events. The two cracks nucleated at the bottom, ruptured together the two desiccated layers, and subsequently propagated bilaterally away from the origin along curved paths. To accommodate the curvature of the paths, coarse en echelon steps or twist hackles intensively developed at the crack peripheries. The two cracks terminate against each other at opposite corners whereas the two other corners are sharp curvatures in the crack planes. These relations suggest that the cracks propagate simultaneously toward each other but intersect in a definite order.

Polygon B has four apparent sides but consists of seven bounded cracks that ruptured together the two desiccated layers. Five of the origins are located at the bottom of polygon B, one at the bottom of polygon A, and one at the bottom of polygon C (arrows in Fig. 4A). The sequential intersection of crack planes is deduced and presented in Figure 4A. Note that an apparent side of polygon B consists of cracks that propagated simultaneously toward each other and terminated in an almost coplanar fashion (Fig. 4A, cracks 4, 4′, and 4″).

For a general view of the number of cracks that bounded certain polygons, I counted the number of all polygons and single cracks that nucleated within an area of ~8 m². I found that the 68 studied polygons were formed by 156 mud cracks. Many of the polygons are bounded by 4 and 5 cracks, but polygons bounded by 2 or 11 cracks are not uncommon (Fig. 6A).

Mud cracks that rupture the set of desiccated layers altogether are older than those that rupture single or multiple desiccated layers. The order of crack formation within individual desiccated layers was established by applying the criteria mentioned herein; however, it was not possible to establish the order of crack formation between different desiccated layers due to the absence of crosscutting relations.

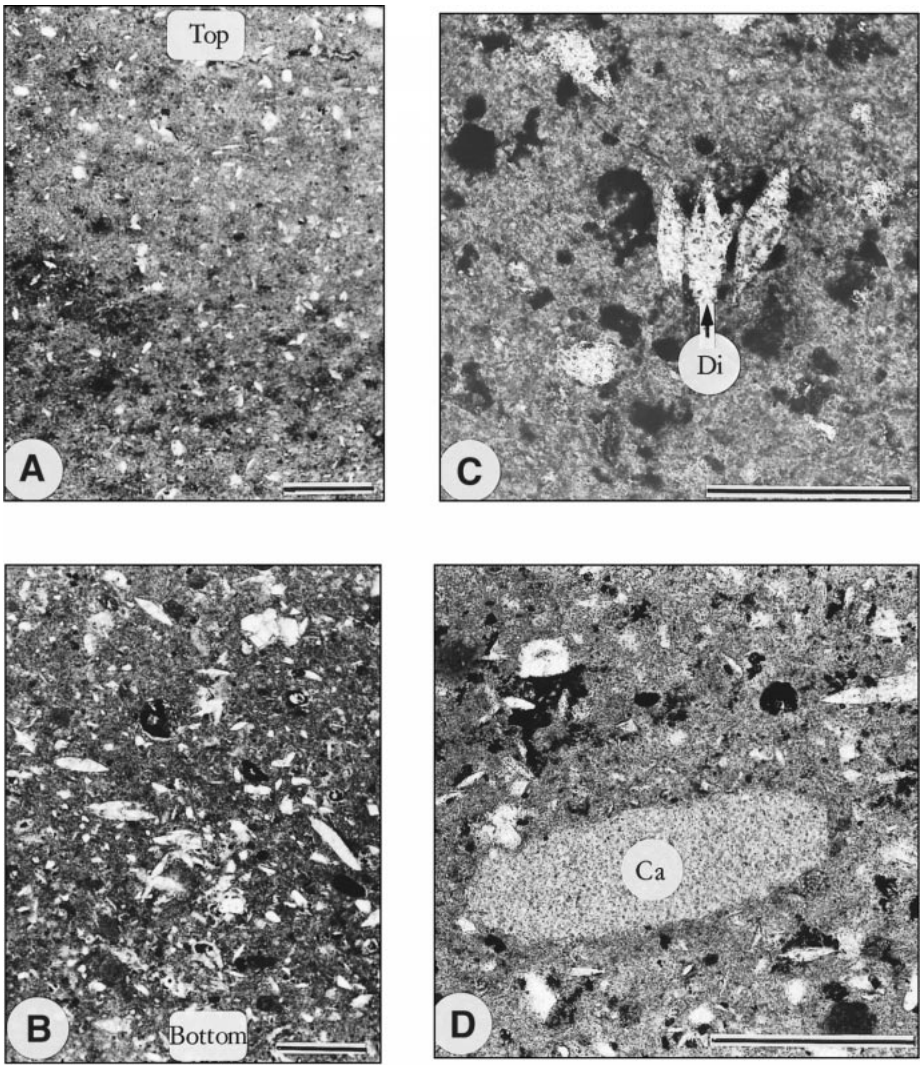

Figure 3. Photomicrographs of the studied mud. Thin sections are oriented parallel to mud-crack planes. Scale bars are 0.5 mm. (A and B) Fining upward of particles (mainly gypsum crystals, chert, and diatoms). The top of desiccation layer 1 seems more homogeneous than the bottom of desiccation layer 2. Distance between bottom of A and top of B is about 30 mm. (C) Closely located diatoms (Di) near the bottom. (D) Well-bonded large eccentric carbonatic particle (Ca) in clay mass.

MECHANICS OF MUD FRACTURING

Effect of Flaw Discontinuities

The consistent location of crack origins at depth strongly suggests that favorable flaws are located near the base of the stratified mud and play a fundamental role during mud-crack nucleation. To test this interpretation, the modifying effect of potential flaws on the distribution of stress in the mud must be examined (Fig. 7). From a microstructure perspective, this examination requires integrating the mechanical formulation presented here into a fracture mechanic formulation that serves to define the conditions whereupon a potential flaw propagates as an opening mode crack (i.e., mud crack). To do so, I draw an analogy between cooling of granular materials and drying of mud. These materials are vulnerable to subfacet defects at grain boundaries, which are probably the most severe flaws leading to mud-crack nucleation. Following Lawn (1993), I approximate a defect as a penny-shaped flaw of radius c_f uniformly stressed by σ^M (Fig. 7, inset). This stress is the superposition of remote tensile stress due to drying, σ_x, and the local mean stress, σ_R, due to elastic mismatch between grains and matrix. In the absence of fluid within the flaw, the critical condition upon which the penny-shaped flaw starts to propagate as an opening mode crack is

$$K_1 = 2\sigma_c^M(c_f/\pi)^{1/2} = 2(\sigma_x + \sigma_R)(c_f/\pi)^{1/2} = R_0, \quad (6)$$

where K_I is the mode-I stress intensity factor,

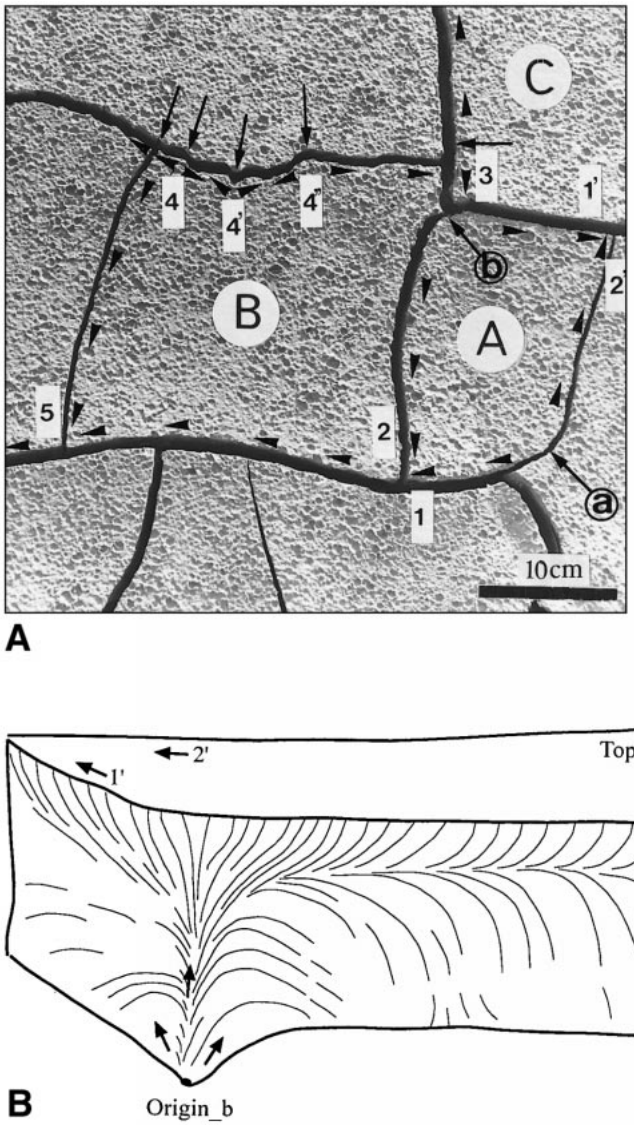

Figure 4. (A) Map view of two adjacent polygons. The number of sides of polygon A is not obvious (three sides? four sides?); this is also true for polygon B (four sides? five sides?). Projection of crack-origin points (indicated by long-tailed arrows) and overall propagation directions (short arrows) are based on interpretation of surface morphology of the associated bounded cracks. Numbers denote the order of crack formation at a given intersection (see text). Polygon A is bounded by only two cracks (denoted a, b). View and interpretation of crack a was presented in Weinberger (1999, Fig. 6 therein). (B) Plumose structures observed in crack b, polygon A, that provide insight into crack evolution. The origin point is located at the convergence point of hackles at the bottom of the desiccated layers. A single vertical plume axis branches into separate subhorizontal axes (along which cracks propagate in opposite directions). The lateral propagation occurred along distinct coplanar fracture surfaces; one fracture, with asymmetric plumose structure, cuts through the lower layer, and a second fracture, with quasisymmetric plumose structure, cuts through the upper layer. These fracture surfaces are slightly noncoplanar, forming an offset of a few millimeters between these surfaces and leaving a delicate step along the boundary. Solid thick lines are hackles. Arrows at the top of the polygon and throughout the polygon show overall propagation directions and local propagation directions, respectively.

R_0 is the grain boundary toughness, and σ_x is given in equation 4. For simplicity, I assume that σ_R is negligible, and equation (6) reduces to the simple form

$$2\sigma_x(c_f/\pi)^{1/2} = R_0. \quad (7)$$

Assume that the microstructure satisfies conditions of geometrical similarity, so that the flaw size c_f scales with the grain size l. In such a case, $c_f = \gamma l$, where γ is a scale-invariant quantity. The prefracture tensile stress in equation 6 is satisfied at the critical grain size (Lawn, 1993, equation 9.8)

$$l_c = \Phi(R_0/\sigma_c^M)^2, \quad (8)$$

where the coefficient $\phi = \pi/4\gamma$ is a dimensionless constant depending on the initial flaw to grain-size ratio.

The analysis in the section on setting and methods indicates that larger grains are more abundant toward the base of the mud due to the natural fining-upward sorting of grains (Fig. 3, A and B). Because the geometrical similarity holds for individual layers, flaws along the bottom of the mud may become critical before flaws that are associated with fine particles at the uppermost desiccation layer, even though the stress due to drying is likely to be less tensile downward. To illustrate this tendency, I calculate the variation of the grain-size ratio l_c/l_{c0} with depth just prior to cracking (where the subscript zero denotes a critical grain size at the surface), assuming that σ_R is negligible and the elastic moduli do not vary much with depth. Under those assumptions, the grain-size ratio is directly related to the moisture content profile (equation 4). Profiles measured by Corte and Higashi (1960, their Fig. 11) show that the moisture content does not differ by more than 2% between the top and bottom part of the soil layer if the thickness is <20 mm. In addition, the moisture content does not differ by more than 10% between the top and bottom part of the 40-mm-thick soil layer just prior to and during cracking. Based on their experiments, I consider a 40-mm-thick layer just prior to cracking with a linear increase in moisture content with depth. The initial moisture content is 60% and the cracking moisture contents at the top and bottom are 25% and 35%, respectively. The difference of 10% should be regarded as an upper limit, as should be the associated tensile stress. The theoretical values of l_c/l_{c0} as a function of depth are less than two near the bottom, while in natural mud may be higher (Fig. 8). This result is in accordance with the interpretation that subfacet defects at grain bound-

aries near the bottom are active sources for mud-crack nucleation.

Similar to cracks in polycrystals (Lawn, 1993), microcracks initiated at grain boundaries might be arrested after extension through several grain diameters. Consequently, contraction during persistent desiccation promotes the flaw severity by further extending the initiated microcracks. For regions near the bottom, the density of microcracking becomes sufficiently high that microcracks coalesce to form a macroscopic mud crack growing from below. Such a mud crack has an activating influence on potential flaws around its front and may restrain other flaws located on either side of it. Thus, evolving mud cracks may play a role in determining the initiation points of subsequent mud cracks. It seems, however, that activated flaws of later generations are also favorably located near the bottom.

Other potential flaws include pores and inclusions. Pores at triple junctions formed by the intersection of grain boundaries are preferred sites for microcracking, tending to be more prevalent in materials with nonuniform grain sizes and composition such as natural mud. They concentrate applied stress over distances that are large compared to a single grain diameter, and therefore are common failure origins (Lawn, 1993). In that sense, the severity of ellipsoidal pores is higher than that of spherical pores, because the former are associated with values of stress concentration factors much higher than the latter. Inclusions with differences in elastic properties between them and the surrounding mud can be even more effective than pores as sources of nucleation. Several possible modes of inclusion-induced cracking based on values of thermal expansion coefficient, elastic modulus, and toughness of particle were depicted in Lawn (1993, his Fig. 9.12). These possibilities include weakly bonded rigid particles that form void-like defects, and contracting, strongly bonded, stiff and tough particles that are associated with radial tensile fractures under applied tension. These possibilities, however, do not account for the size of the flaws, and provide no explanation for preferred nucleation at depth. In linear elastic fracture mechanics the stress concentration around holes and/or inclusions depends on shape rather than size. In real material, however, there is a hole and/or inclusion size effect, whereby strength decreases with increasing size (Anderson, 1997, and references therein). For the studied mud, larger and stiffer inclusions commonly include carbonate and chert grains that preferably settle along the bottom (Fig. 3), and larger pores are expected to be located at triple junctions

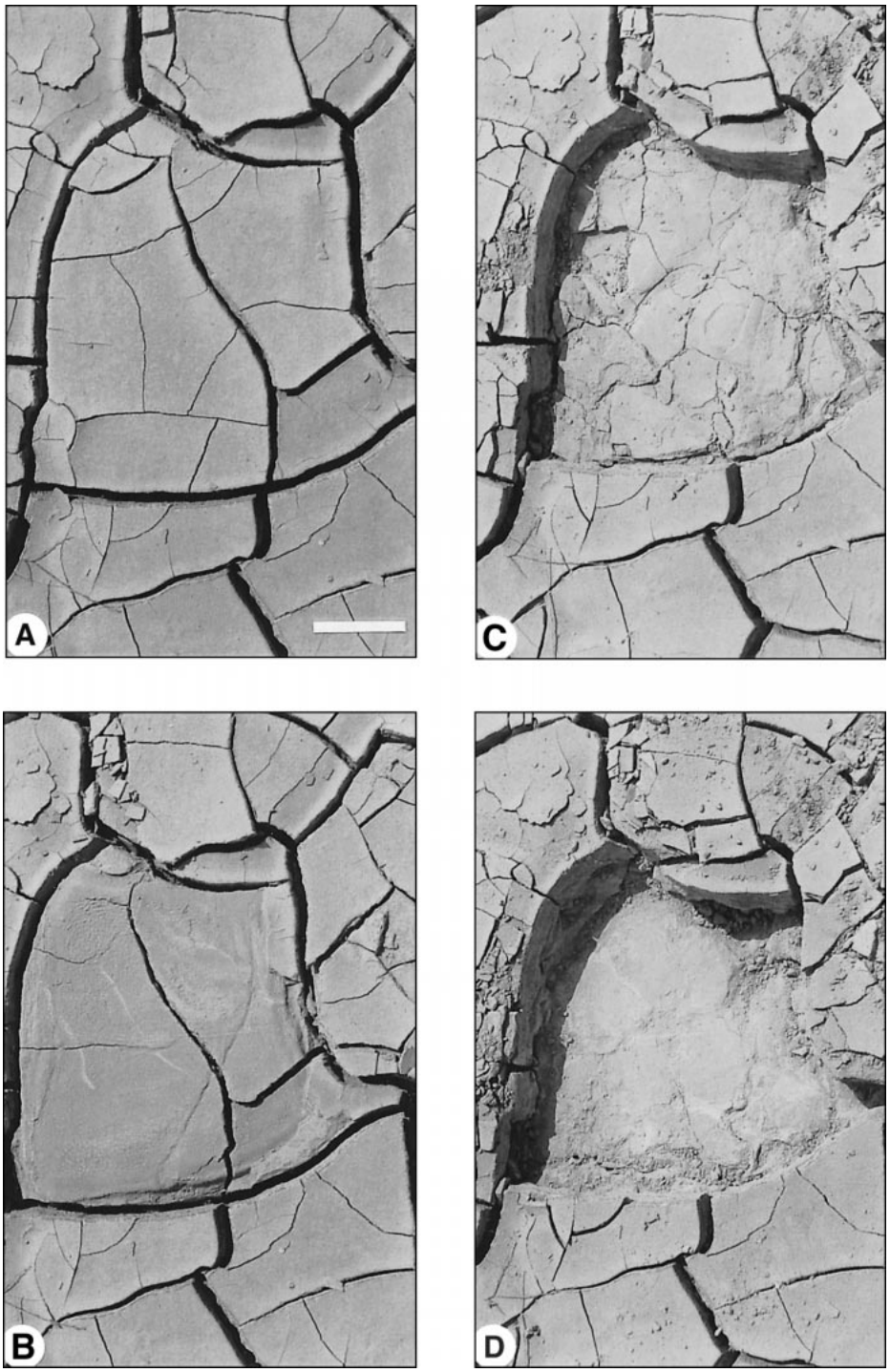

Figure 5. Series of photographs documenting sequential removal of three mud layers from top to bottom of a certain master polygon. Different polygonal patterns are observed in each layer. A few older cracks rupture two or three layers and thus are seen in more than one photograph. (A) Surface pattern (top of third layer) before analysis. (B) Polygonal pattern at the top of second layer after removal of 8-mm-thick layer. Number of secondary polygons is different from that at the surface. (C) Polygonal pattern at the top of first layer after removal of 50-mm-thick layer. (D) Bottom of mud after removal of 22-mm-thick layer. Scale bar is 0.1 m.

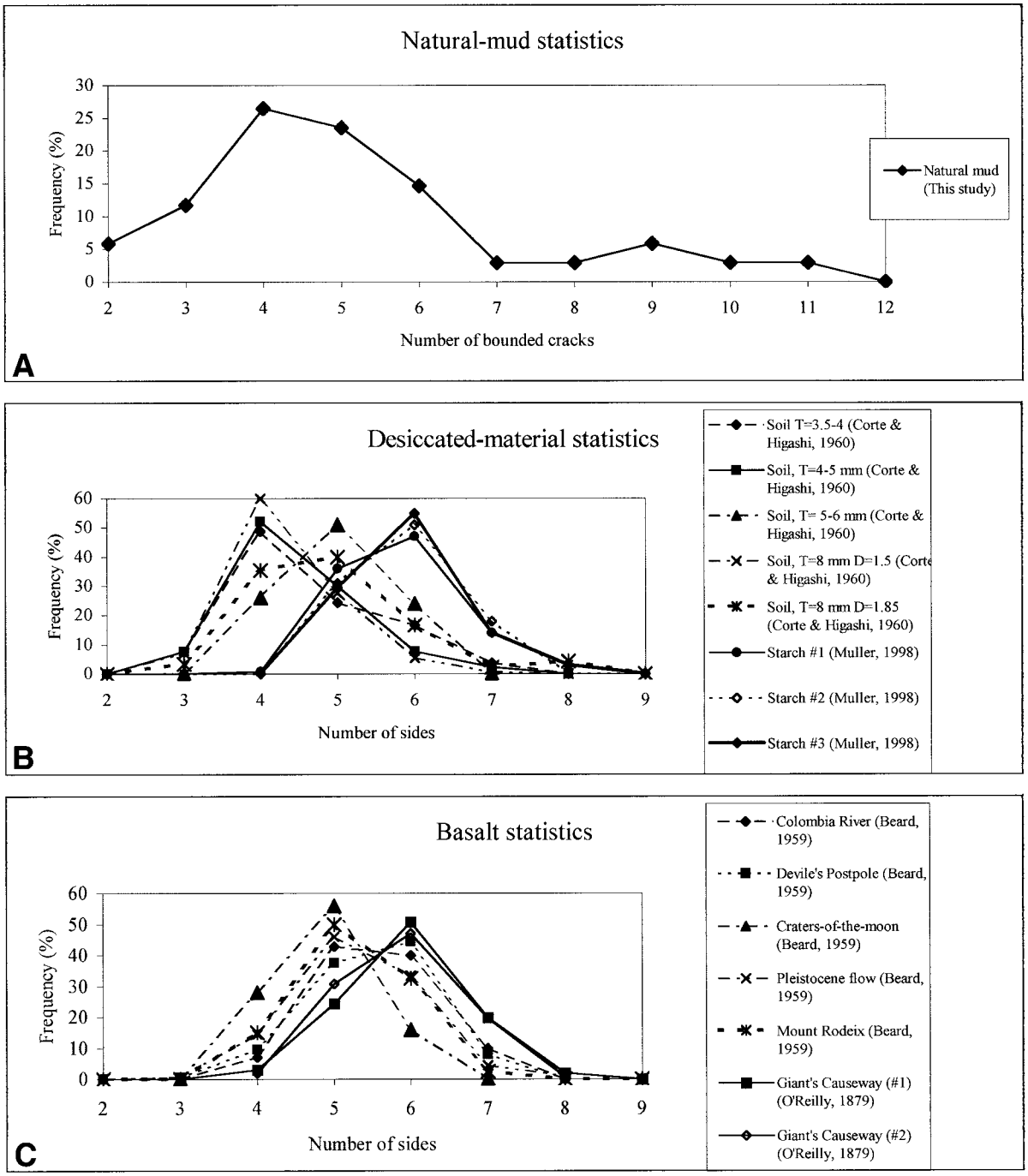

Figure 6. (A) Bounded-crack statistics for mud cracks in a desiccated area ~8 m², Dead Sea region, Israel. Number of analyzed polygons is 68. Note long tail of high values to the right of the distribution (positive skewness). (B) Side statistics of experimental materials of various thicknesses, material properties, and applied conditions. Statistics from Corte and Higashi (1960) are denoted by broken lines; statistics of starch columns from Müller (1998) are denoted by solid lines and represent second-generation desiccation cracks. (C) Side statistics in different basalt column locations (Table 1).

of such grains. Therefore, it is not surprising that such flaws serve as origin points located at depth. This simple analysis suggests that the nonuniform flaw distribution is more important for mud-crack nucleation and growth than the stress variations with depth due to drying and capillary forces. Consequently, the mechanics of fracturing of sediments containing such flaw distribution also support the interpretation that mud cracks commonly nucleate at depth.

Effect of Surface Discontinuities

The bottom of stratified mud defines a discontinuity in the sediment, distinguishing between the fine-grained upper layers that tend to contract and crack, and the coarse-grained lower layers that do not have this tendency. Rainwater is likely absorbed by the upper layers and may not penetrate deeply. Alternatively, the lower layers are relatively permeable and rainwater may pass through them and drain out quickly. In both cases, the bottom marks the level above which favorable flaws are subjected to tensile stress due to drying and polygonal patterns are formed. The moisture content profile, however, might be different for each alternative and does not have a definite influence upon the cracking phenomena (Corte and Higashi, 1960).

In the early stages of desiccation, the adhesion between the layers is high, and they are ruptured as a unit. Thus, early generations of mud cracks form similar polygonal patterns throughout the sequence of desiccated layers. Minor differences might be due to segmentation along layer boundaries and noncoplanar propagation in adjacent layers facilitated by these discontinuities. At later stages of desiccation, the loss of moisture loosens the adhesion between adjacent layers to the extent of delaminating them. Each layer then contracts and cracks separately as the resistance along the layer interfaces diminishes, and cracks do not cross these discontinuities. Consequently, later generations of mud cracks form different polygonal patterns within individual layers. Groisman and Kaplan (1994) demonstrated that decrease in adhesion between coffee-water mixtures decreases the number of cracks and produces different polygonal patterns at the surface. The decrease of adhesion between adjacent layers affects the upper interfaces before affecting the lower ones. Therefore, it appears that later generations of propagating mud cracks consume surface energy derived from the reduction in elastic strain energy caused by delamination of the lower interfaces. However, these cracks have insufficient driving energy to propagate across the delaminated interfaces.

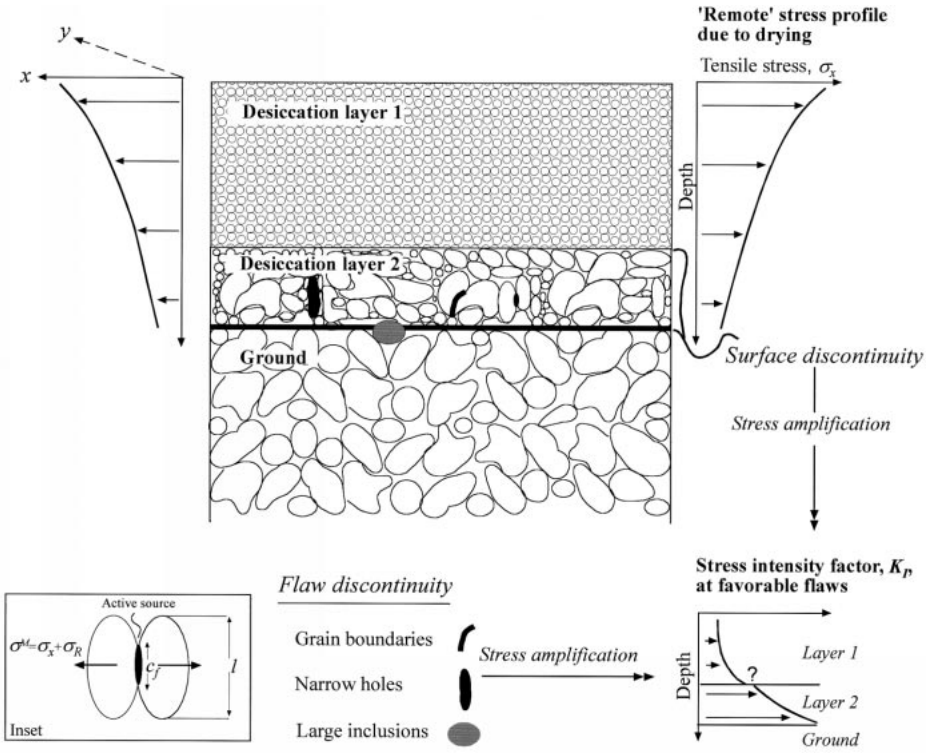

Figure 7. Schematic model of favorable discontinuities (flaws, bedding planes) and the associated stress state prevailing during desiccation (see text for details). Inset: *l*—grain size; c_f—radius of penny-shaped flaw; σ_x—tensile stress due to drying; σ_R—contraction anisotropy stress; σ^M—stress acting on a subfacet defect at grain boundary; K_I—mode-one stress intensity factor.

DISCUSSION

Cracking Induced by Desiccation in Laboratory Experiments and in Nature

Experimental studies of cracking induced by desiccation utilize homogeneous materials of uniform grain size such as starch (Walker, 1986; Müller, 1998), ground coffee (Groisman and Kaplan, 1994), and sieved soil (Corte and Higashi, 1960). Mixtures of these materials with water are commonly poured on glass, PVC, or wood, and then dried and cracked. These studies do not simulate the natural sorting of grains and formation of mud layers, and generally do not account for the sandy substance that often underlies natural mud. In these experiments, discriminated macroscopic flaws are absent and cracks are initiated from inherent inhomogeneities of the mixture. Corte and Higashi (1960) indicated that the moisture-content profile across a vertical section of desiccated materials does not necessarily control where cracks nucleate in the soil. Groisman and Kaplan (1994) argued that friction at the bottom of the mud governs the cracking phenomena, while the nonuniformity of the moisture content profile, if it exists, is not essential for mud cracking. Nevertheless, experimentally induced cracks commonly originate at the top of the desiccated layer (Corte and Higashi, 1960; Müller, 1998). This result shows exactly the opposite of the present field observations, which unambiguously indicate that cracking usually begins at the bottom of layered mud.

Two differences between the experimental and natural setting should be highlighted. First, favorable flaws are concentrated at the base of natural mud, whereas inherent flaws are uniformly distributed throughout the experimental materials. Second, adhesion between natural mud and the underlying sandy material is lower than that between experimental materials and glass, implying that setting the materials over a glass substance inhibits nucleation at the bottom (Corte and Higashi, 1960). The latter point was elaborated in Weinberger (1999); if adhesion between the desiccated mud and the underlying material is higher than the cohesion of the mud

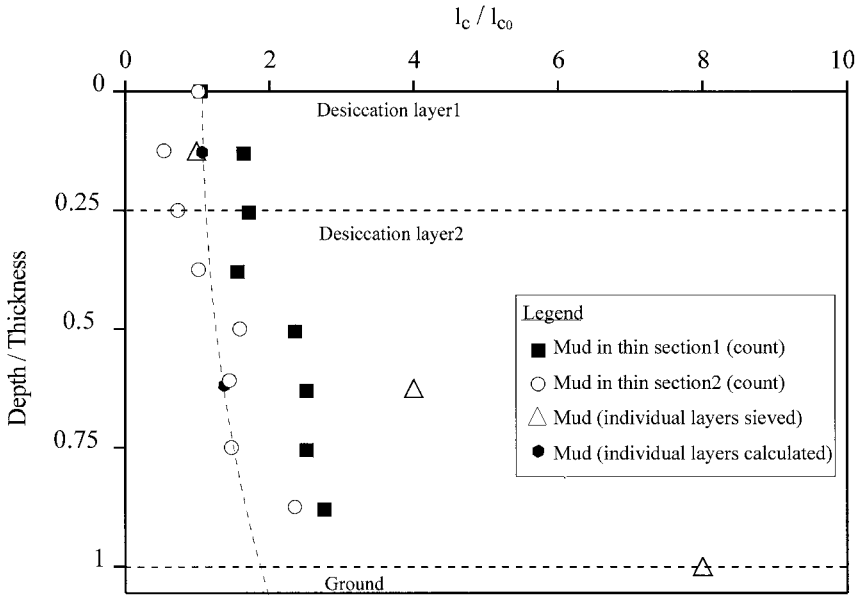

Figure 8. Theoretical variation of critical grain-size ratio l_c/l_{c0} with depth for two individual layers (solid hexagons) having a microstructure that satisfies conditions of geometrical similarity. Calculations are based on text equations 4 and 8 with initial moisture content of 60%, and linear increase of moisture content from top (25%) to bottom (35%) just prior to cracking. Active sources for mud-crack nucleation that are located to the right of the broken line represented an apparent continuous variation l_c/l_{c0} for a 40-mm-thick mud. Measurements of l_{c0} and l_c were made in two representative thin sections of natural mud and correspond to the largest grain size measured along eight horizontal scan lines equally distributed within two 40-mm-thick desiccation layers (counting method). Each thin section samples an area of 15 cm². Measurements of l_{c0} and l_c for the two desiccation layers and ground were obtained by gently disintegrating the grain aggregate and sieving the grains through screens of decreasing mesh size (sieving method). The mud volume used for the analysis of each layer is ~400 cm³. There is a discrepancy between the two methods; the sieving method better represents the actual grain-size distribution than the counting method.

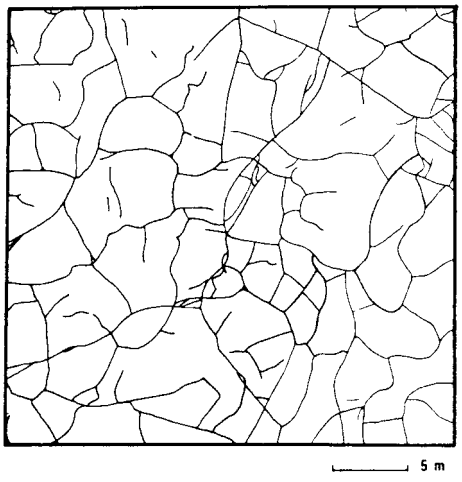

Figure 9. Polygonal pattern at the surface of Alae Lake, Hawaii (after Peck and Minakami, 1968). Contraction cracks are highly curved, limiting rigorous definition of the number of polygon sides.

mass, cracking would start anywhere along the mud column except at the bottom. However, if adhesion along the boundary between the desiccated mud and the underlying material is lower than the cohesion of the mud mass, then cracking might start at any favorable flaw located along or near the bottom. These significant differences between laboratory and nature clearly emphasize that experiments do not adequately simulate the nucleation and growth of natural mud cracks.

At any given intersection, the involved mud cracks form sequentially. A characteristic of this sequence is that new cracks orthogonally approach existing mud cracks. Consequently, cracks seldom propagate along straight paths; e.g., what appear as several polygon sides may actually be a single curviplanar crack (Fig. 4). In such cases, previously suggested relationships between the number of polygon sides and the thickness and material properties of the desiccated layers (Corte and Higashi, 1960) are not always rigorously defined, because recognition of a polygon side is somewhat subjective. A more meaningful relationship is found by comparing the number of polygon-bounding cracks with the layer thickness. Figure 6 presents the frequency distribution of the number of polygon sides from several experiments and materials, as well as that of the bounded cracks in the studied natural mud. Regardless of the type of material used, or its thickness or moisture content, the majority of experimentally induced polygons have four to seven sides. The natural polygons, however, are most frequently associated with 3 to 7 bounded cracks, but may be bounded by as many as 11 cracks. The wide range of bounded-crack frequencies suggests, in part, that single sides of a polygon do not always coincide with single bounded cracks.

The hexagonality index χ_6 of polygonal patterns can be used to describe the deviation of a distribution of sides and/or bounded cracks from the expected value of 6 (equation 9; Budkewitsch and Robin, 1994). Similarly, the pentagonality index χ_5 of polygonal pattern describes the deviation of the distribution from the value of 5:

$$\chi_6 = [(f_5 + f_7) + 4(f_4 + f_8) + 9(f_3 + f_9) + 16(f_2 + f_{10}) + 25f_{11} + \cdots]^{/2}$$

$$\chi_5 = [(f_4 + f_6) + 4(f_3 + f_7) + 9(f_2 + f_8) + 16f_9 + 25f_{10} + .36f_{11} + \cdots]^{/2}, \quad (9)$$

where f_n is the fraction of an n-sided crack-bounded polygon. I calculate these indexes for natural mud (the present data sets), experimentally utilized soil (Corte and Higashi 1960, their Figs. 28, 39, 40), starch specimens (Müller, 1998, his Fig. 2A), and observed polygonal patterns in basalts (Budkewitsch and Robin, 1994, their Table 2). The calculated indexes are given in Table 1 and display the following characteristics. (1) Hexagonality and pentagonality indexes for natural mud deviate strongly from indexes determined for starch, soil, and basalts. (2) Indexes for the starch specimens are very similar to those calculated from polygonal patterns in basalts, in agreement with the analogy suggested by Müller (1998). (3) Indexes for desiccated soils indicate that the evolving patterns are closer to pentagonal than to any other shape. The high values of hexagonality and pentagonality indexes calculated for polygonal patterns in natural mud are attributed to the long tail of high values to the right (positive skewness, Fig. 6A), making the median of the distribution less than the mean. This analysis indicates

TABLE 1. DISTRIBUTION OF THE POLYGON SIDES/BOUNDED CRACKS IN NATURAL MUD, DESICCATED MATERIALS, AND BASALT INTERIOR

Sample	References	Number of polygon sides/bounded cracks										Sample size	N	χ_6	χ_5
		2	3	4	5	6	7	8	9	10	11				
Natural mud	This study	4	8	18	16	10	2	2	4	2	2	68	5.18	2.66	2.13
Starch specimen #1	Müller (1998)	0	0	1	36	46	14	3	0	0	0	100	5.82	0.81	1.14
Starch specimen #2	Müller (1998)	0	0	0	31	51	18	0	0	0	0	100	5.87	0.90	1.11
Starch specimen #3	Müller (1998)	0	0	0	44	82	20	4	0	0	0	150	5.89	0.73	1.15
Compact soil	Corte and Higashi (1960)	0	14	118	54	11	1	0	0	0	0	198	4.33	1.82	0.97
Loose soil	Corte and Higashi (1960)	0	11	118	134	55	7	14	0	0	0	339	4.90	1.50	1.05
Soil, thickness of 3.5–4 mm	Corte and Higashi (1960)	0	8	54	27	18	4	0	0	0	0	111	4.60	1.69	1.04
Soil, thickness of 4–5 mm	Corte and Higashi (1960)	0	12	79	45	12	3	0	0	0	0	151	4.43	1.77	1.00
Soil, thickness of 5–6 mm	Corte and Higashi (1960)	0	0	22	42	20	0	0	0	0	0	84	4.97	1.24	0.71
Devil's Postpole, basalt	Beard (1959)	0	1	29	92	67	9	2	0	0	0	200	5.30	1.08	0.87
Columbia River Basalt	Beard (1959)	0	0	5	30	28	7	0	0	0	0	70	5.53	0.90	0.93
Giant's Causeway, basalt	O'Reilly (1879)	0	0	6	49	102	40	4	0	0	0	201	5.94	0.80	1.23

that the larger range of the present data set should not be discarded and may be of mechanical significance, as discussed in the following section.

Is Mud Fracturing Analogous to Basalt Fracturing?

Based on theoretical considerations and some similarity of crack patterns, an analogy has been drawn between fracturing of mud and basalt (e.g., Price and Cosgrove, 1994). The limitations of this analogy are discussed here by comparing the observations of DeGraff and Aydin (1988) in basalt with those of this study in natural mud. In basalt, cracks nucleate at the exterior regions of the solidifying magma where the thermal stress due to cooling is concentrated (e.g., by vesicles). Inward propagation of cracks into hotter regions is limited by the decrease in thermal stress. Consequently, a basalt column face is the net result of many discrete fracture events, each of which produces a well-defined segment of the face (Ryan and Sammis, 1978; DeGraff and Aydin, 1988). Thus, at a given level, each column side is formed by a single bounded crack, and side statistics of the basalt interiors are identical to bounded crack statistics. Polygonal patterns characterized by curved boundaries occur at the flow surface (Fig. 9; Peck and Minakami, 1968), where the thermal stress parallel to this surface is strongly anisotropic and where lava is highly heterogeneous (DeGraff and Aydin, 1988). Hexagonal joint networks occur in flow interiors, where the absence of surface effects and the homogeneity of lava produces a relatively isotropic horizontal thermal stress. Conversely, in natural mud, cracks may systematically nucleate at the heterogeneous base of the drying mud, where the tensile stress due to drying is amplified at favorable flaw and surface discontinuities. Incremental upward propagation of cracks into the dryer regions is facilitated by increase in tensile stress and capillary forces. Crack networks at the mud surface show complex patterns and are strongly related to the evolving cracks from the heterogeneous base of natural mud.

In summary, basalt and natural mud have opposed propagation directions of cracks with respect to the top of the cooling flow or drying mud, but similar polygonal patterns at the surface of these materials (cf. Figs. 4A and 9). However, polygonal patterns in natural mud are different from those developed in basalt interiors, as indicated by the difference in the hexagonality and pentagonality indexes (Table 1). As for the experiments, I attribute this difference to the difference in the level of material heterogeneity between natural mud and basalt interior. In the former, crack nucleation and growth appear to be strongly related to the nonuniform distribution of macroscopic flaws within the mud, and cracks cannot simply arrange themselves in hexagonal and pentagonal patterns, as do cracks in homogeneous basalt interiors.

Counting the number of polygon-bounding cracks is a tedious task compared to counting polygon sides. In many cases, it is also impossible to count the number of polygon-bounding cracks due to the two-dimensional nature of the outcrops and the lack of diagnostic plumose structures. Nevertheless, counting cracks is an objective procedure, while recognition of polygon sides is a subjective poorly defined procedure. The pattern of cooling cracks on the surface of Alae Lake, Hawaii, clearly shows this problem (Fig. 9). Previous studies (e.g., Budkewitsch and Robin, 1994) characterized the progressive evolution of columnar joints by counting the number of polygon sides and defining a relation between the number of polygon sides and the thickness and properties of the desiccated layer (e.g., Corte and Higashi, 1960). It would appear that the more meaningful number of polygon-bounding cracks would provide a better model; however, this study shows that in some cases the two numbers are similar. This suggests that the number of polygon sides may provide a first-order approximation for the well-defined number of polygon-bounding cracks.

Implications for Sedimentology

The downward-tapering shape of mud cracks has commonly been interpreted to reflect the downward growth of mud cracks (Selley, 1976). According to this view, mud cracks are not necessarily terminated at the same level in the mud mass, but at different depths. This study, however, provides an alternative view, in which mud cracks may terminate at the same level because they nucleate at depth and subsequently propagate upward, rupturing the desiccated layers. In mechanical terms, the downward-tapering shapes of mud cracks, where present, are related to the volumetric change with depth, and not necessarily related to the crack-propagation direction. This has important implications for the significance of mud cracks in ancient sedimentary rocks. The shape of mud cracks should not simply serve as a way-up criterion (top versus bottom of a stack of layers; see Weinberger et al., 1997), and should not be regarded as an indicator for the crack-propagation direction. Indeed, I observed ancient mud cracks of Neogene age that terminate at the top and bottom of the mud layer (Fig. 10), in agreement with the mechanism of incipient crack formation in modern mud, inferred herein.

CONCLUSIONS

1. Mud cracks may systematically nucleate at or near the bottom of a fining-upward mud; they subsequently propagate vertically upward toward the free surface and laterally outward toward adjacent cracks.

2. Earlier generations of mud cracks form

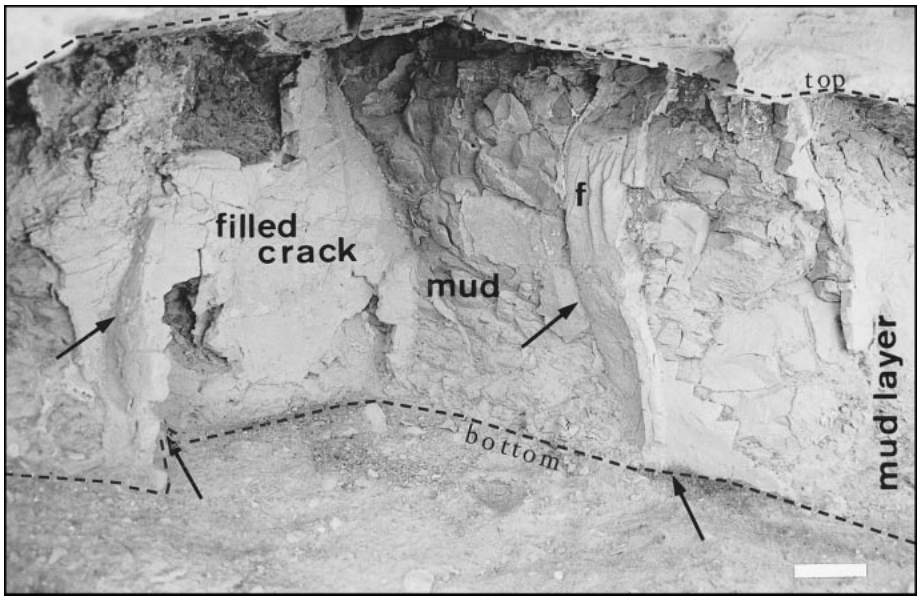

Figure 10. Cross section of ancient filled mud cracks (Neogene age) in Hazeva Formation, Rahas Wadi, southern Israel. Cracks terminate at the top and bottom of the mud (marked by broken line). Orthogonal intersections are indicated by arrows. Curious fingering (f) is imprinted at the surface of the cracks, interpreted as an indication of silt filling from the top. Scale bar is 0.1 m.

polygonal patterns that are similar throughout the mud layers. Later generations of mud cracks fracture each mud stratum separately, forming different polygonal patterns at individual levels.

3. The consistent location of crack origins at the bottom of the polygons indicates that origin flaws (grain boundaries, narrow holes, and inclusions) may favorably locate along the base and play a fundamental role during mud-crack nucleation.

4. Observations of nucleation and upward propagation suggest that the distribution of favorable flaws more strongly influences the fracture process than stress variations with depth due to loss of moisture.

5. Cracking is restricted by the adhesion between the desiccated layers and the underlying substance. This restriction causes elastic energy to be stored, and, at a critical level, used to create a new crack surface. The decrease of adhesion between adjacent desiccated layers during persistent desiccation causes cracks to be confined between delaminated horizons.

6. A simple mechanical model shows that subfacet defects at grain boundaries near the base may become critical before defects associated with fine particles at the top, even though the stress profile due to drying is usually more tensile at the top.

7. Counting and sieving methods indicate that grain boundaries at the bottom are several times longer than at the top of the mud due to the natural sorting of grains, illustrating the validity of the model.

8. Experimental studies of cracking induced by desiccation do not simulate well the mechanism of natural mud-crack formation because they utilize homogeneous materials of uniform grain size and artificial bottom substances.

9. The number of polygon sides is not rigorously defined, whereas the number of single cracks that bound individual polygons is well defined.

10. The analogy between fracturing of natural mud and fracturing of basalt interior is limited because there are significant differences in the degree of homogeneity of these materials.

ACKNOWLEDGMENTS

I am grateful to Vladimir Lyakhovsky for useful discussions during the course of this study, and to Amihai Sneh, who introduced me to the remarkable mud cracks in the Hazeva Formation. I thank David Soudry and Shimon Ilani for their assistance in the petrographic and mineralogical determinations. Comments and reviews by Gerhard Müller, Mark Fischer, Rebecca Dorsey, and an anonymous reader led to significant improvements in the paper. I gratefully acknowledge the field assistance of Moshe Arnon and the style editing by Ximena Wdowinski. This study was partially supported by grant 9800198 from the United States–Israel Binational Science Foundation, Jerusalem, Israel.

REFERENCES CITED

Allen, J.R.L., 1985, Principles of physical sedimentology: London, George Allen and Unwin, 272 p.

Anderson, T.L., 1997, Fracture mechanics: Fundamentals and applications: Boca Raton, Florida, CRC Press, 688 p.

Aydin, A., and DeGraff, J.M., 1988, Evolution of polygonal fracture patterns in lava flows: Science, v. 239, p. 471–476.

Bahat, D., 1991, Tectonofractography: Berlin, Springer-Verlag, 354 p.

Bahat, D., and Engelder, T., 1984, Surface morphology on cross-fold joints of the Appalachian Plateau, New York and Pennsylvania: Tectonophysics, v. 104, p. 299–313.

Baldwin, C.T., 1974, The control of mud crack patterns by small gastropod trails: Journal of Sedimentary Petrology, v. 44, p. 695–697.

Beard, C.N., 1959, Quantitative study of columnar jointing: Geological Society of America Bulletin, v. 70, p. 379–382.

Begin, Z.B., Nathan, Y., and Ehrlich, A. 1974, Lake Lisan, the Pleistocene precursor of the Dead Sea: Israel Geological Survey Bulletin 63, 30 p.

Budkewitsch, P., and Robin, P.Y., 1994, Modelling the evolution of columnar joints: Journal of Volcanology and Geothermal Research, v. 59, p. 219–239.

Corte, A.E., and Higashi, A., 1960, Experimental research on desiccation cracks in soil: US Army Snow, Ice and Permafrost Research Establishment Report 66, 48 p.

DeGraff, J.M., and Aydin, A., 1988, Surface morphology of columnar joints and its significance to mechanics and direction of joint growth: Geological Society of America Bulletin, v. 99, p. 605–617.

Groisman, A., and Kaplan, E., 1994, An experimental study of cracking induced by desiccation: Europhysics Letters, v. 25, p. 415–420.

Gross, M.R., 1993, The origin and spacing of cross joints: Examples from the Monterey Formation, Santa Barbara coastline, California: Journal of Structural Geology, v. 15, p. 737–751.

Grossenbacher, K.A., and McDuffie, S.M., 1995, Conductive cooling of lava: Columnar joint diameter and striae width as functions of cooling rate and thermal gradient: Journal of Volcanology and Geothermal Research, v. 69, p. 95–103.

Helgeson, D.E., and Aydin, A., 1991, Characteristics of joint propagation across layer interfaces in sedimentary rocks: Journal of Structural Geology, v. 13, p. 897–911.

Ji, S., and Zhao, P., 1994, Strength of two-phase rocks: A model based on fiber-loading theory: Journal of Structural Geology, v. 16, p. 253–262.

Kranz, R.L., 1983, Microcracks in rocks: A review: Tectonophysics, v. 100, p. 449–480.

Kulander, B.R., Barton, C.C., and Dean, S.L., 1979, Application of fractography to core and outcrop investigations: U.S. Department of Energy Paper METL/SP-79/3, 174 p.

Lachenbruch, A.H., 1962, Mechanics of thermal contraction cracks and ice-wedge polygons in permafrost: Geological Society of America Special Paper 70, 69 p.

Lawn, B., 1993, Fracture of brittle solids: London, Cambridge University Press, 378 p.

Müller, G., 1998, Starch columns: Analog model for basalt columns: Journal of Geophysical Research, v. 103, p. 15239–15253.

Müller, G., and Dahm, T., 2000, Fracture morphology of tensile cracks and rupture velocity: Journal of Geophysical Research, v. 105, p. 723–738.

Neal, J.T., Langer, A.M., and Kerr, P.F., 1968, Giant desiccation polygons of Great Basin playas: Geological Society of America Bulletin, v. 79, p. 69–90.

Olson, J.E., and Pollard, D.D., 1989, Inferring paleostresses from natural fracture patterns: A new method: Geology, v. 17, p. 345–348.

O'Reilly, J.P., 1879, Explanatory notes and discussion on

the nature of the prismatic forms of a group of columnar basalt, Giant's Causeway: Royal Irish Academy Transactions, v. 26, p. 641–728.
Peck, D.L., and Minakami, T., 1968, The formation of columnar joints in the upper part of Kilauean lava lakes, Hawaii: Geological Society of America Bulletin, v. 79, p. 1151–1166.
Piggott, M.R., 1991, Failure processes in the fiber-polymer interface: Composites Science and Technology, v. 42, p. 57–76.
Plummer, P.S., and Gostin, V.A., 1981, Shrinkage cracks: Desiccation or synaeresis?: Journal of Sedimentary Petrology, v. 51, p. 1147–1156.
Pollard, D.D., and Aydin, A., 1988, Progress in understanding jointing over the past century: Geological Society of America Bulletin, v. 100, p. 1181–1204.
Price, N.J., and Cosgrove, J.W., 1994, Analysis of geological structures: New York, Cambridge University Press, 502 p.
Ryan, M.P., and Sammis, C.G., 1978, Cyclic fracture mechanics in cooling basalt: Geological Society of America Bulletin, v. 89, p. 1295–1308.
Scott, R.F., 1963, Principles of soil mechanics: London, Addison Wesley, 550 p.
Selley, R.C., 1976, An introduction to sedimentology: New York, Academic Press, 408 p.
Turcotte, D.L., and Schubert, G., 1982, Geodynamics—Application of continuum physics to geological problems: New York, John Wiley, 450 p.
Walker, J., 1986, Cracks in a surface look intricately random but actually develop rather systematically: Scientific American, December, p. 178–183.
Weinberger, R., 1999, Initiation and growth of cracks during desiccation of stratified muddy sediments: Journal of Structural Geology, v. 21, p. 379–386.
Weinberger, R., Agnon, A., and Ron, H., 1997, Paleomagnetic reconstruction of a diapir emplacement: A case study from Sedom diapir, Dead Sea rift: Journal of Geophysical Research, v. 102, p. 5173–5192.

MANUSCRIPT RECEIVED BY THE SOCIETY JUNE 16, 1999
REVISED MANUSCRIPT RECEIVED JANUARY 13, 2000
MANUSCRIPT ACCEPTED FEBRUARY 16, 2000

Printed in the USA